

# Numerical crack modelling of tied concrete columns under compression

C. Bosco and S. Invernizzi\*

*Dipartimento di Ingegneria Strutturale e Geotecnica, Politecnico di Torino, Torino, Italy*

*(Received September 14, 2010, Revised March 15, 2012, Accepted March 19, 2012)*

**Abstract.** In the present paper the problem of monotonically compressed concrete columns is studied numerically, accounting for transverse steel reinforcement and concrete cracking. The positive confinement effect of the ties on the core concrete is modeled explicitly and studied in the case of distributed or concentrated vertical load. The main aim is to investigate the influence of transverse reinforcement steel characteristics on the column load carrying capacity and ductility, in order to provide an evaluation about some standards requirements about the class and ductility of steel to be used for ties. The obtained results show that the influence of transverse reinforcement steel class of ductility is negligible both on the column load carrying capacity and on its ductility. Also the dissipated energy is basically unchanged. In view of these evidences, some standards requirements about the steel class of ductility to be used for ties appear to be rather questionable.

**Keywords:** smeared cracking; tied concrete columns; confinement.

---

## 1. Introduction

It is well known that, when particular collapse mechanisms are taking place in the structure, the concrete columns must provide not only a given strength but also the necessary ductility in order to allow for sufficient energy dissipation without a sensible reduction of the bearing capacity. This becomes crucial in the case of seismic repeated loading.

The ductility of concrete columns is basically a function of the concrete class of resistance, of the amount and mechanical characteristics of the longitudinal reinforcements, as well as of the amount, characteristics and position of the transverse reinforcement, i.e., the ties. The ties provide a level of confinement of the column concrete core that depends also on the shape of the column cross-section (e.g. circular or rectangular). In recent years, several authors carried out experimental tests, e.g. (Hong *et al.* 2006, Hwang and Yun 2004), and some prescriptions have also been incorporated in National Standards (e.g. EC8, ACI 318 and NZS 3101).

In the present paper the results of a set of finite element numerical simulations are presented. The numerical analyses have been carried out with the commercial finite element code DIANA9.3. The presence of transverse reinforcement has been explicitly taken into account, allowing for the assessment of the influence of the ties arrangement. In the present case, perfect-bonding special embedded reinforcement elements have been used. In addition, no-bonding or a given shear-slip law can be considered for the reinforcement. Thanks to a smeared crack approach based on total strain,

---

\* Corresponding author, Ph.D., E-mail: [stefano.invernizzi@polito.it](mailto:stefano.invernizzi@polito.it)

it has been possible to simulate numerically the crack pattern, included the ability to model the spalling of concrete parts outside the confined core.

Some of the experimental results available in the literature concern columns loaded on a limited area of the cross section. This aspect has been considered in details, since many convergence difficulties arise in this case. In fact, at the border of the loaded area the classical discontinuities of contact mechanics are detected in the stress and displacement fields. Moreover, in the transition zone the finite element reach a critical condition both for compression and tension (and cracking), with the consequent local instabilities. This problem has been overcome adopting a spring bedding in correspondence of the loaded area.

Furthermore, it has been investigated the influence of tie class of ductility on the overall ductility of the column. This aspect is particularly relevant to some European country where the National Standards ask for some questionable ductility requirements for the transverse reinforcement.

In general, the proposed numerical approach provides a way for the interpretation of the experimental results and a valuable strategy for the study and design of non-standard cases.

## 2. Experimental evidences

When the load is applied to the structure acting on a very limited area (concentrated load) a transition zone (discontinuity) can be recognized, where a complex three-dimensional stress state takes place. In this case (Fig. 1), three main critical areas can be considered. The region right below the loaded area, characterized by high compressive stresses; the region aligned with the load axis, characterized by tensile tractions (*bursting stresses*) that tend to split the element, and the surface region around the loaded area, also subjected to tensile stresses which are responsible for surface cracking and possible expulsion of material (*spalling*).

The phenomenon was firstly analyzed by Morsch (1924) who introduced the strut and tie model. The approach was based on the equilibrium of internal forces (compression or traction) with linearized trajectories. In this way, it is possible to calculate the resultant of the tractions normal to the external load, i.e., the bursting force. In the fifties, Guyon (1953) provided a theory based on the analogy of the symmetric prism, and on the fotoelasticity experimental results of Tesar (1932). In later time, those results were also confirmed numerically by Yettram (1969).

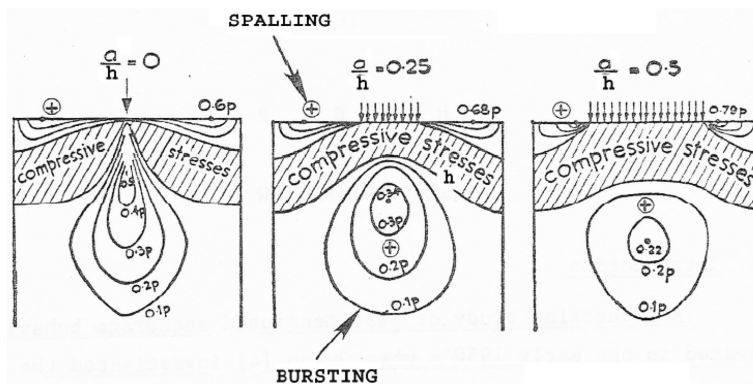


Fig. 1 Fotoelasticity results obtained by Tesar (1932)

Given the bursting force  $Z$ , which is the integral of tensile stresses, it is possible to design the tie reinforcement that has to be put in place to avoid the splitting of the element region close to the concentrated load. The influence of tie reinforcement distribution was studied by Adeghe and Collins (1986) by means of a nonlinear finite element calculation. They emphasized that if the reinforcement is not adequately smeared over the splitting region, the behavior can be quite fragile. In addition, they showed that due to the limited diffusion of stresses allowed in the nonlinear analysis, with respect to the linear one, the position of the bursting force is closer to the loaded area and, therefore, the reinforcement area has to be increased.

In more recent times it has been recognized that the effect of the transversal reinforcement is not limited to sustain the tensile forces that originate below the loaded area, but pertain also a favorable three-dimensional compressive stress state of the concrete below the loaded area (Fig. 2). This effect has been accounted for both in the CEN (2004) Eurocodes and in the CEB-FIB (1993) Model Code, by means of empirical expressions for the increased strength and increased ultimate strain.

The increased ultimate strain, i.e., ductility, plays a crucial role especially in the case of the seismic resistance of columns. This effect has been investigated experimentally by several authors.

Madner *et al.* (1988) considered circular and rectangular cross section columns, varying the amount of transverse reinforcement. They emphasized that in addition to the increase of the compressive strength and ultimate deformation, the tie reinforcement provides a great increase of the dissipated energy.

Sheikh and Uzumeri (1980), considering concrete with a cylindrical strength comprised between 30 MPa and 40 MPa, noted that the positive effect of confinement takes place starting from a mean axial deformation of 0.0015. If the deformation is increased, the inner concrete core carries increasing stresses, while the outer part progressively unload. At a deformation of approximately 0.004, the outer concrete is spalled off from the column. The use of smooth rebars does not influence sensibly the behavior of the columns, since the spalling of the outer concrete vanishes the exchange of shear stresses between steel and concrete. On the other hand, a key role is played by the tie arrangement, which can sensibly improve the confinement in rectangular cross section columns.

In recent years, the effect of confinement in self-compacting and or high strength concrete has also been investigated (Khayat *et al.* 2001). In this case, the positive confinement effect is less sensible due to the limited Poisson's coefficient.

Finally, experimental results have been made available about the confinement of concrete with

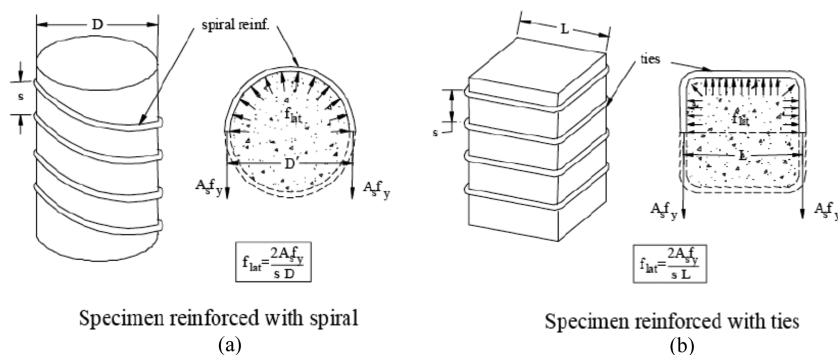


Fig. 2 Scheme of the concrete confinement with circular (a) and rectangular ties (b)

fiber-reinforced composites (Karantzikis *et al.* 2005).

Numerical simulations have been carried out by Gao *et al.* (2011), Pandey and Benipal (2011), Philip (2009) and Mirzabozorg *et al.* (2009).

### 3. Monotonic compression of columns

The numerical simulations have been carried on considering a square concrete column 600 mm by 600 mm, with 1200 mm height. A regular quadratic brick element mesh was adopted. Four concentrated load configurations have been considered (Fig. 3) in addition to distributed load.

Embedded reinforcement has been added to the mesh (Fig. 4). Two different arrangements were considered: square ties and square ties with additional reinforcement ligaments between the tie midpoints.

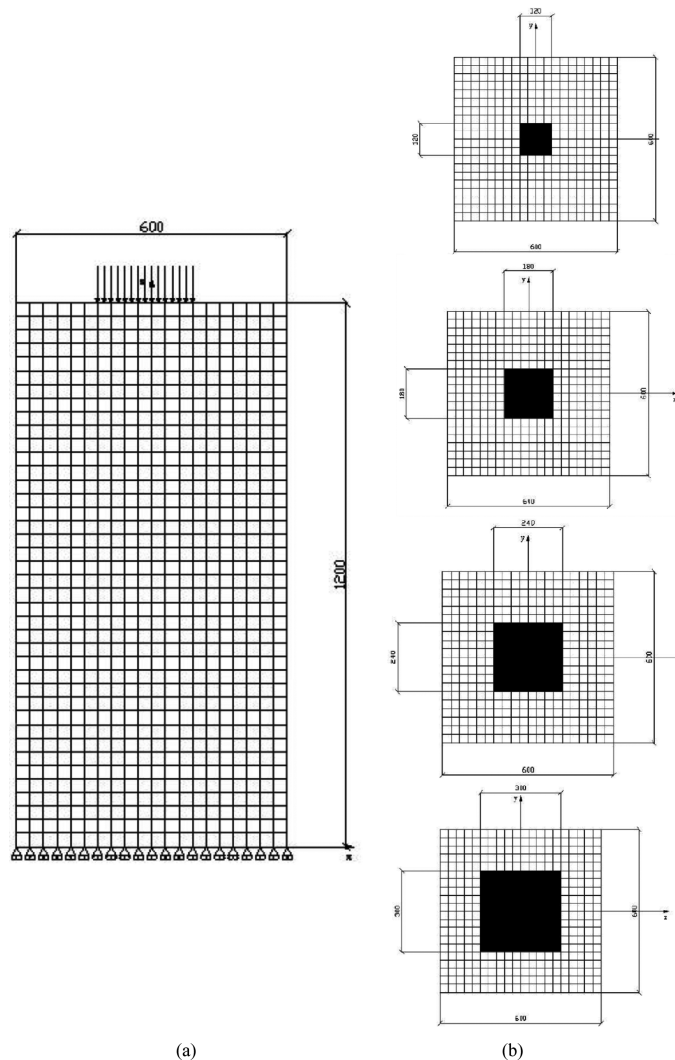


Fig. 3 Geometry of the column (a) examples of different loaded areas and (b)  $a/d=0.2, 0.3, 0.4$  and  $0.5$

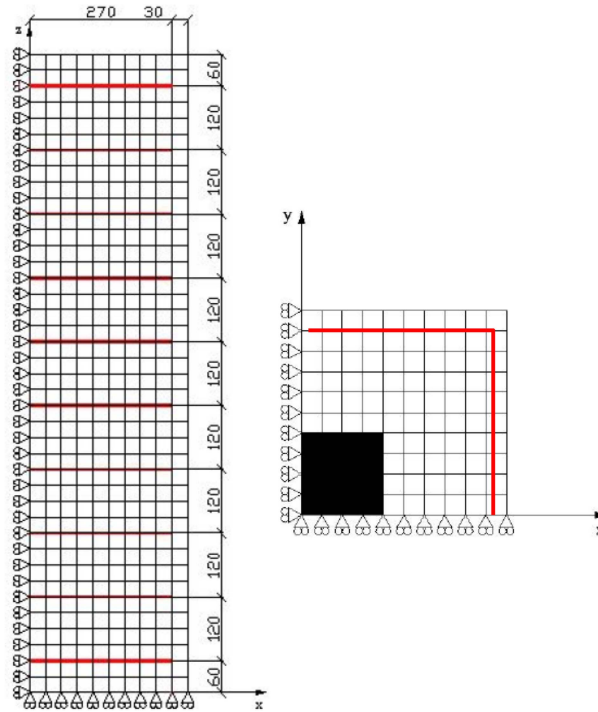


Fig. 4 Discretization mesh obtained exploiting symmetry and position of the ties

### 3.1 Compressive behavior of concrete

Concrete subjected to compressive stresses shows a pressure-dependent behavior, i.e., the strength and ductility increase with increasing isotropic stress. Due to the lateral confinement, the compressive stress-strain relationship is modified to incorporate the effects of the increased isotropic stress. Furthermore, it is assumed that lateral cracking influences the compressive behavior. To model the lateral confinement effect, the parameters of the compressive stress-strain function,  $f_c$  and  $\varepsilon_p$ , are determined with a failure function which gives the compressive strength as a function of the confining stresses in the lateral directions.

The base function in compression can be modeled with a number of different curves, included the Thorenfeldt and the parabolic curve. The class of the concrete used in the analyses was C30.

#### 3.1.1 Lateral confinement

The increase of the strength with increasing isotropic stress is modeled with the four-parameter Hsieh-Ting-Chen failure surface, which is defined as

$$f = 2.0108 \frac{J_2}{f_{cc}^2} + 0.9714 \frac{\sqrt{J_2}}{f_{cc}} + 9.1412 \frac{f_{c1}}{f_{cc}} + 0.2312 \frac{I_1}{f_{cc}} - 1 = 0 \quad (1)$$

with the invariants  $J_2$  and  $I_1$  defined in terms of the stress in the concrete, and  $f_{c1}$  the maximum principal stress (DIANA 2008). The parameters in Eq. (1) can be determined by fitting of experimental data on concrete specimens. The effect of confinement is shown in Fig. 5, for different ratios between axial and lateral pressure.

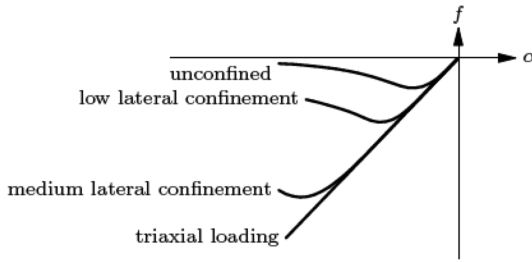


Fig. 5 Influence of lateral confinement on compressive stress-strain curve (DIANA 2008)

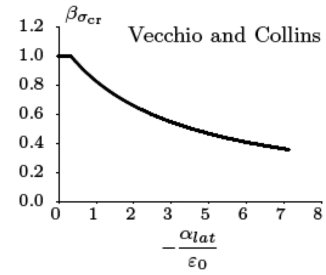


Fig. 6 Peak stress reduction factor due to lateral cracking (DIANA 2008)

### 3.1.2 Lateral cracking

In cracked concrete, large tensile strains perpendicular to the principal compressive direction reduce the concrete compressive strength. The compressive strength is consequently not only a function of the internal variable in a certain direction, but also a function of the internal variables governing the tensile damage in the lateral directions. If the material is cracked in the lateral direction, the strength parameters are reduced with the factor  $\beta_{\epsilon_{cr}}$  for the peak strain, and with the factor  $\beta_{\sigma_{cr}}$  for the peak stress, which are functions of the average lateral damage variable.

The relationship for reduction due to lateral cracking is the model according to Vecchio and Collins (1993), shown in Fig. 6.

### 3.2 Cracking of concrete

The behavior of concrete subjected to tension has been modeled with the smeared cracking approach. A formulation based on the so-called *total strain crack model* was adopted (DIANA 2008), which combine the tensile and compressive behavior in a unique relationship. This constitutive model is based on the Modified Compression Field Theory, originally proposed by Vecchio and Collins (1986). Due to the amount and disposition of the reinforcement in the columns under consideration, the coaxial concept was adopted, which allows for a rotation of the crack set following the principal stress redistribution. The behavior of concrete in tension is linear up to the reaching of the tensile strength (in the present case  $f_t = 2.9$  MPa), while the post peak behavior is linear (Fig. 7).

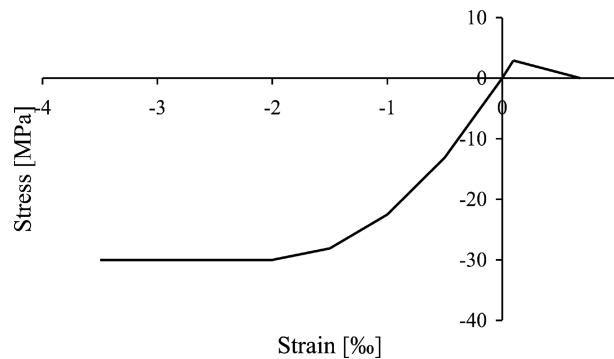


Fig. 7 Stress-strain constitutive law for concrete

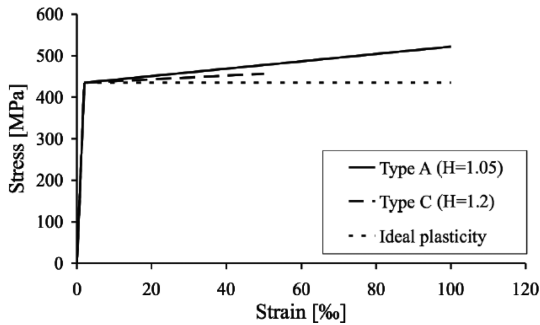
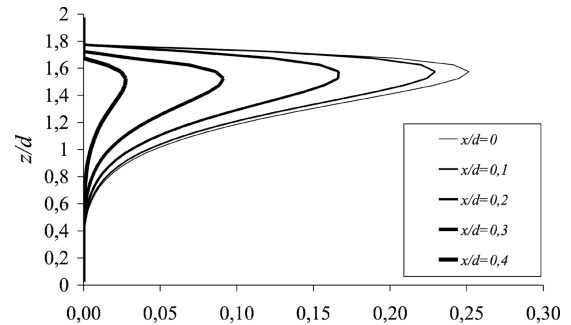


Fig. 8 Bilinear constitutive law for reinforcement steel


 Fig. 9 Normalized tensile stresses (in the  $y$  direction) versus normalized height ( $z/d$ ). Diagram along the symmetry axis ( $x/d=0$ ) and approaching the column surface ( $x/d \rightarrow 0.5$ )

### 3.3 Reinforcement

As far as the reinforcement is concerned, a bilinear constitutive law was adopted. The initial linear part of the diagram is characterized by a Young's modulus  $E_s=200$  GPa, up to the yielding stress  $f_y=435$  MPa. Three different case have been considered for the inelastic part, namely: perfect plasticity, 1.2 linear hardening up to the limit deformation of 10% (representative of type C steels) and 1.05 linear hardening up to the limit deformation of 5% (representative of type A steels). The constitutive laws for steel are shown in Fig. 8.

## 4. Numerical results

When the load is applied on a limited loading area, many convergence difficulties can arise. In fact, at the border of the loaded area the classical discontinuities of contact mechanics are detected in the stress and displacement fields. In addition, in the transition zone the finite element reach a critical condition both for compression and tension (and cracking), with the consequent local instabilities. This problem has been overcome adopting a spring bedding in correspondence of the loaded area.

### 4.1 Plain concrete

The first set of simulations has been carried on taking into consideration a plain concrete column. Six different loading area ratios are studied, namely  $a/d=0.2$ ,  $a/d=0.3$ ,  $a/d=0.4$ ,  $a/d=0.5$ ,  $a/d=0.6$  and  $a/d=0.7$ .

Three main reference longitudinal deformations are chosen to represent the stress state in the column (the deformation of the elastic bedding was not considered), 0.2%, 2% and 5% respectively. In particular, 0.2% is chosen as a reference to the initial loading range.

Fig. 9 shows the evolution of tensile stress, in the  $y$  direction, along the  $z$ -axis for  $a/d=0.5$ . The curves are calculated starting from the symmetry axes ( $x/d=0$ ), and approaching the surface of the column ( $x/d \rightarrow 0.5$ ).

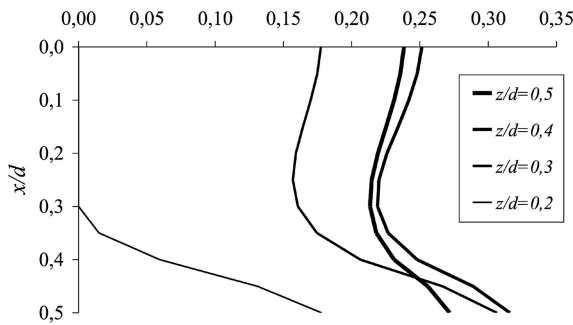


Fig. 10 Normalized tensile stresses (in the  $y$  direction) versus normalized abscissa ( $x/d$ ). Diagrams for increasing normalized depth ( $z/d$ )

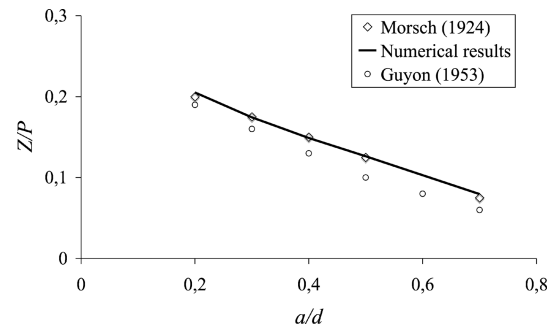


Fig. 11 Comparison between the normalized bursting force ( $Z/P$ ) obtained numerically and the results from Morsch (1924) and Guyon (1924) for different load ratios ( $a/d$ )

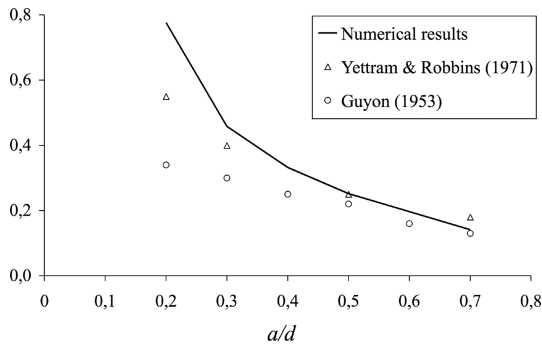


Fig. 12 Normalized maximum bursting tensile stress as a function of the loaded area ( $a/d$ )

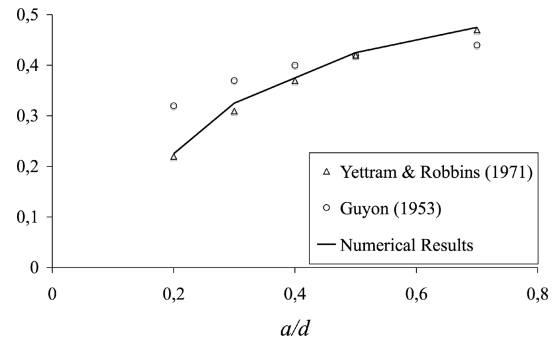


Fig. 13 Comparison between the normalized positions of the bursting force, and results from Yettram and Robbins (1971) and Guyon (1953)

On the other hand, Fig. 10 shows how the tensile stress varies along the  $x$ -axis with reference to different relative depth. Stresses are normalized with respect to the nominal vertical stress.

The two diagrams agree with the experimental results from photoelasticity (Tesar 1932) and with the numerical results obtained by Yettram (1969).

The integration of the tensile stress field over a vertical section of the column provides the bursting force  $Z$ . Fig. 11 compares the magnitude of the numerical bursting force normalized with respect to the applied axial force  $P$ , with the empirical results from Morsch (1924) and Guyon (1953).

In Fig. 12 the comparison is shown between the maximum tensile stresses. Fig. 13 shows the comparison considering the position of the tensile stress resultant. It can be noticed that the numerical calculation generally provides higher values of the maximum tensile stress, while the resultant is often located closer to the loaded area.

As the mean deformation of the column increase, it is possible to observe the migration of tensile stresses due to the cracking and damage below the loaded area. This phenomenon can be clearly detected in the diagram of Fig. 14.

In addition, the magnitude of the bursting force first increases for increasing deformations, and



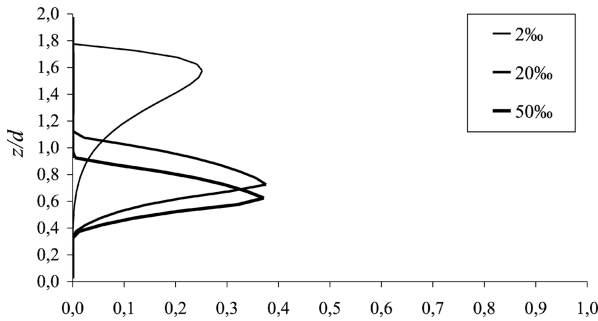


Fig. 14 Migration of the normalized principal tensile stresses (calculated on the symmetry axis) away from the loaded area ( $a/d=0.5$ )

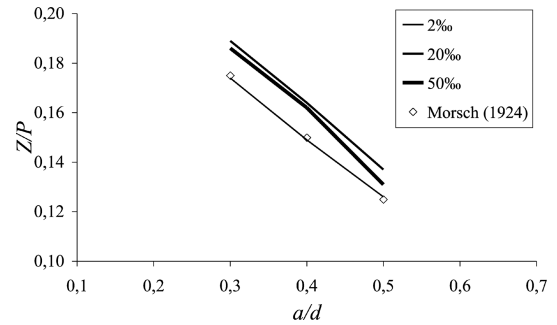


Fig. 15 Bursting force for increasing mean deformations of the column, for different loaded areas compared with Morsch (1924)

then decreases (Fig. 15). With this respect, it is also interesting to note that the Morsch (1924) prevision is more accurate for low levels of deformation.

#### 4.1.1 Square ties

When ties are added to the column, the damage below the loaded area is greatly limited. Due to the presence of transverse reinforcement an almost constant region bearing the tensile stresses takes place (Fig. 16). In addition, in the lower part of the column the horizontal stresses become negative, providing a favorable three-dimensional stress state.

This phenomenon can be confirmed looking at the confinement stresses in Fig. 17 that shows the second principal component of stress, calculated on the symmetry axis. The curves are oscillating due to the tie spacing. The minimum stresses (i.e., maximum confinement effect) are reached in correspondence of the positions of the ties.

The axial stress in the transverse reinforcement is shown in Fig. 18, where the abscissa equal to zero refers to the tie midpoint, while 270 mm is the tie corner. It is not possible to appreciate any sensible difference when different types of steel are used.

The same behavior appears in term of the load bearing capacity of the column (Fig. 19). Therefore, it can be said that an improved ductility class of steel does not provide a valuable

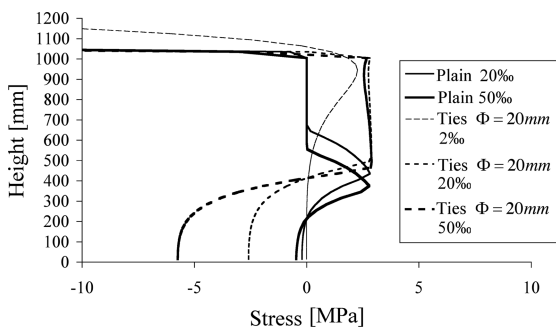


Fig. 16 First principal tensile stress (on the symmetry axis): comparison between the plain and reinforced case ( $a/d=0.5$ )

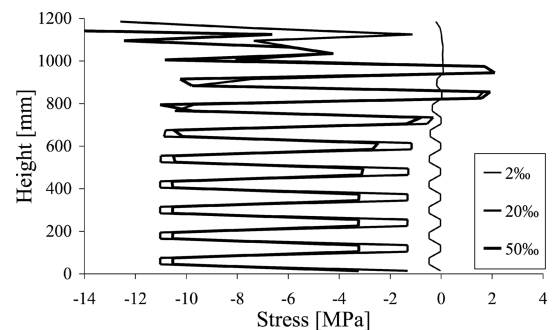


Fig. 17 Confinement stresses in correspondence of increasing mean column deformation. The oscillations correspond to the tie spacing

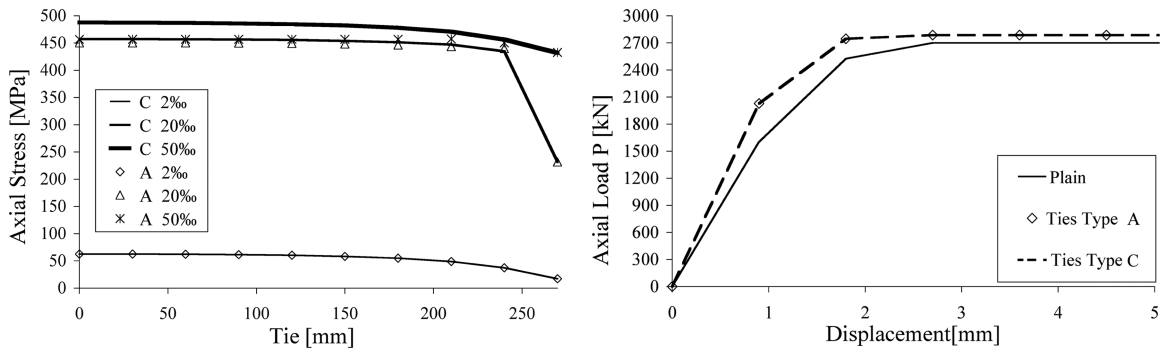


Fig. 18 Evolution of the stress state in the ties (steel Fig. 19 Load displacement curve: plain concrete, reinforcement type A and reinforcement type C

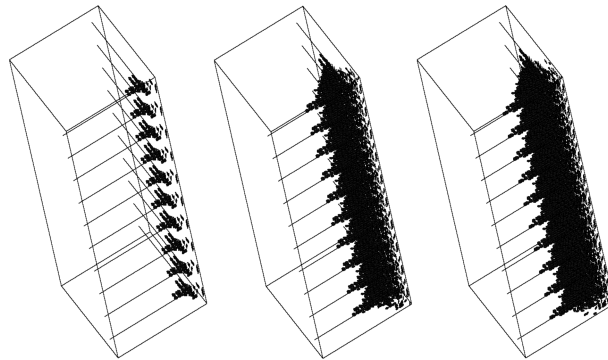


Fig. 20 Evolution of the crack pattern in one quarter of the column

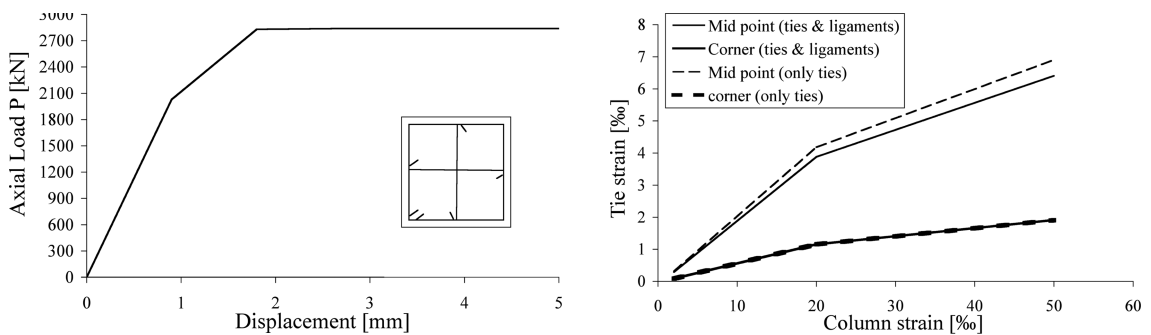


Fig. 21 Load displacement curve in the case of ties Fig. 22 Tie strain decrease due to additional ligaments with additional ligaments

additional strength and ductility, nor dissipated energy.

Fig. 20 shows the evolution of the crack pattern. It is well recognizable the spalling mechanism which affects the outer region of the concrete column.

#### 4.1.2 Square tie with additional ligaments

When the ties arrangement is changed, e.g. adding two additional ligaments between the tie

midpoints, the confinement effect is sensibly improved. This can be appreciated in term of load bearing capacity and dissipated energy (Fig. 21).

A quantitative assessment can be obtained also considering the magnitude of tensile stresses in the tie in the two cases (Fig. 22). On the other hand, the effect of the tie steel class of ductility is negligible.

## 5. Conclusions

A numerical study of the problem of monotonically compressed concrete columns has been presented, accounting for transverse steel reinforcement and concrete cracking. The positive confinement effect of the ties on the core concrete has been modeled explicitly and studied in the case of distributed or concentrated vertical load. In this way, the proposed numerical approach provides a tool for the interpretation of the experimental results and a valuable strategy for the study and design of non-standard cases.

The obtained results show that the influence of transverse reinforcement steel class of ductility is negligible both on the column load carrying capacity and on its ductility. Also the dissipated energy is basically unchanged. In view of these evidences, some standards requirements about the steel class of ductility to be used for ties appear to be rather questionable.

## References

- Adeghe, L.N. and Collins, M.P. (1986), *A finite element model for studying reinforced concrete detailing problems*, Department of civil engineering, University of Toronto, 86-12.
- CEB-FIP (1993), *Model code 1990*, CEB Bulletin No. 213-214, Lausanne.
- CEN (2004), *Eurocode 2: Design of concrete structures*, Brussels, Ref. No. EN 1992-1-1:2004: E.
- Gao, H.Y., Guo, X.L. and Hu, X.F. (2011), "Crack identification based on Kriging surrogate model", *Struct. Eng. Mech.*, **41**(1), 25-41.
- Guyon, Y. (1953), *Prestressed concrete*, John Wiley and Sons, New York.
- Hong, K.N., Han, S.H. and Yi, S.T. (2006), "High-strength concrete columns confined by low-volumetric-ratio lateral ties", *Eng. Struct.*, **28**(9), 1346-1353.
- Hwang, S.K. and Yun, H.D. (2004), "Effects of transverse reinforcement on flexural behaviour of high-strength concrete columns", *Eng. Struct.*, **26**(1), 1-12.
- Karantzikis, M., Papanicolaou, C.G., Antonopoulos, C.P. and Triantafillou, T.C. (2005), "Experimental investigation of nonconventional confinement for concrete using FRP", *J. Compos. Constr.*, **9**(6), 480-487.
- Khayat, K.H., Paultre, P. and Tremblay, S. (2001), "Structural performance and in-place properties of self-consolidating concrete used for casting highly reinforced columns", *ACI Mater. J.*, **102**(4), 560-568.
- Mander, J.B., Priestley, M.J.N. and Park, R. (1988), "Observed stress-strain behavior of confined concrete", *J. Struct. Eng.-ASCE*, **114**(8), 1827-1849.
- Mirzabozorg, H., Kianoush, R. and Jalalzadeh, B. (2009), "Damage mechanics approach and modeling nonuniform cracking within finite elements for safety evaluation of concrete dams in 3D space", *Struct. Eng. Mech.*, **33**(1), 31-46.
- Pandey, U.K. and Gurmail S. Benipal (2011), "Bilinear elastodynamical models of cracked concrete beams", *Struct. Eng. Mech.*, **39**(4), 465-498.
- Philip, P. (2009), "A quasistatic crack propagation model allowing for cohesive forces and crack reversibility", *Interact. Multiscale Mech.*, **2**(1), 31-44.
- Sheikh, S.A. and Uzumeri, S.M. (1980), "Strength and ductility of tied concrete columns", *J. Struct. Div.-ASCE*, **106**(5), 1079-1102.

- Tesar, M. (1932), "Détermination expérimentale des tensions dans les extrémités des pièces prismatiques munies d'une semi-articulation", Abh IVBHI.
- Vecchio, F.J. and Collins, M.P. (1986), "The modified compression field theory for reinforced concrete elements subjected to shear", *ACI J.*, **83**(22), 219-231.
- Vecchio, F.J. and Collins, M.P. (1993), "Compression response of cracked reinforced concrete", *J. Struct. Eng.-ASCE*, **119**(12), 3590-3610.
- Yettram, A.L. (1969), "Anchorage zone stresses in axially post-tensioned members of uniform rectangular section", *Mag. Concrete Res.*, **21**(67), 103-112.

CC